Biochar based tin-oxide nanocomposite for remediation of water

Vipin Kaswan*, *Maha* Saleem, *Harpreet*

Lovely Professional University, Phagwara, Punjab-144411, India
*Corresponding author: agand2010@gmail.com

Abstract. In the present scenario, pure drinking water is a great problem. Scientists are finding out ways to combat this problem. Various approaches are being used for water remediation, but there is always a need to get more economical, eco-friendly and viable method for removal of pollutants from water. In the present study, an attempt have been made to prepare composite (RHAC/SnO_2) from biochar from rice husk and SnO_2. The comparison of adsorption and photo catalysis for removal of methylene blue (MB)has been done. It was concluded that biochar is efficient in removal of MB by adsorption at all the tested pH, whereas SnO_2 has removed 75% MB by adsorption at pH 10. The RHAC/SnO_2 composite was found to be a better adsorbent of MB with 90% efficiency, whereas its photocatalytic activity was less with 61% efficiency at pH 10. The present findings need to be further explored so as to get a better insight of the prepared composite.

INTRODUCTION

As we know in today's world's biggest problem is purified drinking water, as industries grow, they produce increased waste and dumpit in rivers, lakes, or empty land, in industrial waste, there is a huge amount of hazardous chemicals that affect fresh water, it produces several diseases to living beings. To lessen these pollutants, including surfactants, metal ions, dyes, and other organic compounds in water, several approaches have been devised and put to use such as reverse osmosis (RO), Advanced oxidation process, adsorption, and ion - exchange. But most of them are expensive and while conventional treatment methods are effective, they can result in secondary contamination that needs to be disposed of further. The adsorption process is ridiculously cheap and easy to do. agricultural waste—activated carbon generated from, for example, *(Mahamad et al.,2015)*, banana peels *(Nguyen et al.,2020)*, rice husk *(Lv et al., 2020)*, and soybean root *(Guo et al.,2016)*.

The ideal material for the adsorption of organic contaminants is activated carbon because of its well-developed porous structure, wide surface area, low density, and strong adsorption capabilities.Additionally, activated carbon has been applied in several other cutting-edge fields, including pharmaceuticals, electrode materials, air filters, and gas storage. As a result, there will be a rise in the price of activated carbon (USD 3.44 billion in 2021), prompting many researchers to look for the cheapest source of the material.

There is a lot of waste biomass, such as straw or leftovers from the manufacture of olive oil and other agricultural goods, and it is sometimes not disposed of in an environmentally acceptable manner. Due to its inexpensive purchase price and the fact that it must frequently be disposed of anyhow, the notion develops to use waste biomass as the foundation material to make activated carbon.On a commercial basis, wood, anthracite and bituminous charcoal, lignite, peat moss, and coconut are the most typical sources of activated carbon. Almond and olive shells are also utilized as substitute supplies. These materials range in carbon content (weight) from 40 to 90% and have a density of 0.4 to 1.45 g/ml. *(Huang et al.,2016; Khadhri et al., 2019; Cui et al.,2011)*. The raw material used to make activated carbon should be widely available, affordable, and secure. This substance should have a low mineral content and little biodegradability when first stored.*(Jolly et al.,2006)*, the raw material used to make activated carbon should be accessible, affordable, and secure. This material's mineral content and biodegradability during initial storage should be as low as possible. *(Prauchner et al., 2016; Samsuri et al.,2014)*

EXPERIMENTAL

Preparation of Rice Husk-ActivatedCarbon (RHAC)

Dried rice husk pieces were subjected to pyrolysis. 60ml of 25%(w/w) $ZnCl_2$solution was added to 15g of rice husk biomass(impregnation ratio 1:1). The resulting mixture was left for 22hrs and dried at 373K for 2hrs. Pyrolysis of the above mixture was done at 853K with an average rate of 10Kmin^{-1} (starting temperature 295K) and held for 2hrs under

continuous flowing N_2 at 1psi. The activated carbon so produced was poured into distilled water and pH was adjusted to 7 using 1M HCl with vigorous stirring and recovered after filtration and drying at 378K.

Preparation of Methylene Blue Solution

About 0.025 g of methylene Blue ($C_{16}H_{18}N_3SCl.3H_2O$) was taken in a 500mL volumetric flask. The final concentration of methylene blue was maintained at $0.05mg^{-ml}$.

Preparation of Tin Oxide Nanoparticles and Tin Oxide Loaded on RHAC

For the synthesis of RHAC/SnO_2composites, 0.75M of oxalic aciddihydrate ($C_2H_2O_4.H_2O$) was added drop by drop to the solution of 0.5M $SnCl_2.2H_2O$ for 1hr on continuous stirring. 0.2g of RHAC was added to this mixture and the resultant solution was kept at 60°C for 4hr under continuous stirring. Finally, the washed and dried material was annealed in a muffle furnace at 400°C for 2hr *(Ramamoorthy et al., 2020).*

Adsorption and Photocatalytic Study

Experiments in batch mode were carried out at room temperature. An adsorption study was conducted for MB removal by RHAC, pure SnO_2, and SnO_2/RHAC.The study was done at three pH viz 3, 7 and 10, and the pH of the solution was adjusted with 0.1M NaOH or 0.1M HCl. For photocatalytic study was carried out with tungsten lamp for 180 minutes, the catalyst dosage of 40 mg in 10 ml for a 50 mg/L solution of methylene blue (MB).

Using a Shimadzu UV-1800 spectrophotometer, the methylene blue solution was monitored every 30 minutes between 0 and 180 minutes. Equation 2 calculated the % removal of dye degradation.

$$\% \, Removal = \frac{C_\circ - C_t}{C_\circ} \, X \, 100 (1)$$

Where C_o = initial concentration of dye(mg/L) and C_t = concentrations at different interval(mg/L)

RESULTANDDISCUSSION:

Characterization:

Morphological analysis

Using a high-energy electron beam to scan the sample, scanning electron microscope pictures of the sample are captured. Atoms and electrons in the sample interact to provide signals that provide details about the surface topography. Figure 1,showsSEM image depicting the well-developed micropore structure of zinc chloride-treated activated carbon of rice husk.Figure

2, shows the SEM image of SnO_2/RHAC well-loaded of nanoparticles on RHAC. Figure 3 shows pure SnO_2

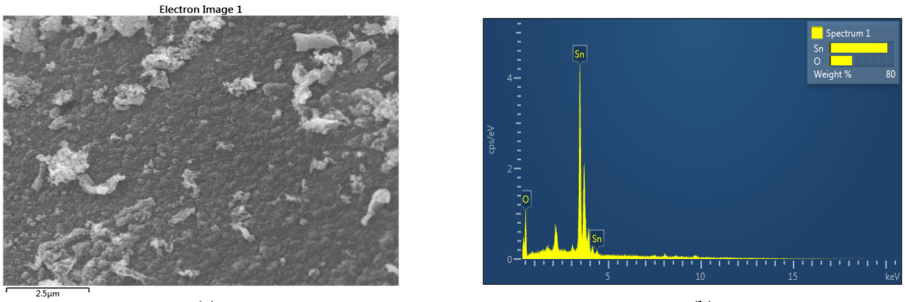

(a) (b)

Figure 1:FE-SEM image of pure tin oxide

nanoparticles SEM image have spherical crystalline. Tables 1,2, and 3 shows the presence of the O, C, Sn, and Si was verified by EDS spectra.[27]

TABLE 1: EDS data of Pure tin oxide (SnO_2)

Spectrum 1	Wt%	Wt% Sigma
O	28.21	0.96
Sn	71.79	0.96
Total	100.00	

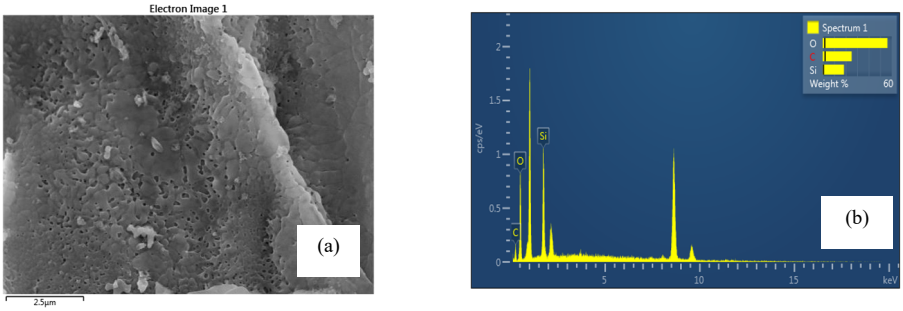

Figure 2:FE-SEM image of RHAC

TABLE 2: EDS Data of RHAC

Spectrum 1	**Wt%**	**Wt% Sigma**
C	25.20	2.19
O	56.28	1.83
Si	18.53	0.76
Total	100.00	

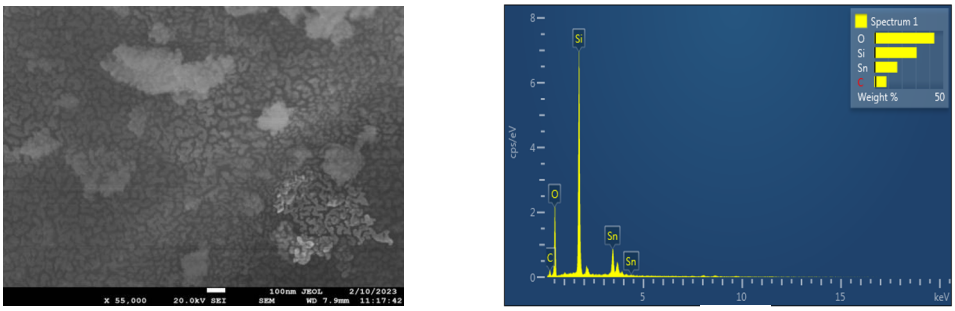

(a) (b)

FIGURE3:(a) FE-SEM image (b) EDS mapping of SnO_2/RHAC

TABLE 3: EDS data of SnO_2/RHAC

Spectrum 1	**Wt%**	**Wt% Sigma**
C	8.90	1.08
O	43.55	0.76
Si	30.78	0.52
Sn	16.77	0.45
Total	100.00	

(i) FTIR study

The FT-IR spectra of pure SnO_2, SnO_2/RHAC, and RHAC composites are shown in Figure 4. RHAC shows the peak at 1075, 980, 866, 574, and 459 cm^{-1} representing the Si-O-Si group and Si-H group (Kaur et al.,2020). The SnO_2/RHAC shows peaks at 1048, 466, and 604 cm^{-1} representing the C-O bond, O-Sn-O blendingand Sn-O stretching vibration. [28]

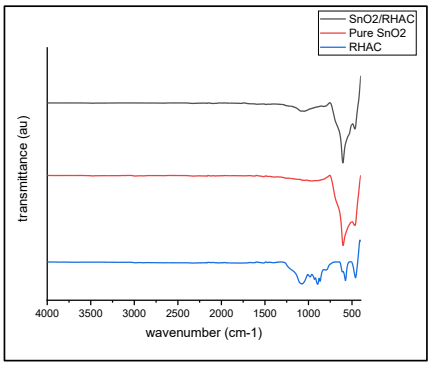

FIGURE4: FTIR spectra of SnO_2/RHAC, pure SnO_2, and RHAC

(ii) XRD Study

The SnO_2 /RHAC and pure SnO_2showed 2θ at 26.6° (110), 33.9° (101), 38.9° (200), 39° (111), 51.8° (211), 54.7° (220), 57.8° (002), 61.9° (310), 64.7° (112) 66° (301) 71.3° (202), and 78.7° (321).A rutile tetragonal structure might be attributed to all of the diffraction peak patterns. While RHAC peaks appear at 2θ 12.6°(110), 22.07°(300), 25.54°(220), 31.53° (113), 34°(410), 38.8°(223), 49.9°(342), 65.6°(713).A rhombohedral structure could be indexed to all of these diffraction patterns. Using Debye Scherrer's formula in equation 1, the crystalline size of the SnO_2/RHAC and pure SnO2 composites was determined. *(Al-Saadi et al.,2019)*. The crystalline size of pure SnO_2 was 26.3nm while SnO_2/RHAC was 17.05nm respectively. As a result, particle sizes are smaller than pure SnO_2 NPs when loaded on RHAC because the crystal structures are constrained. Due to restrictions on its development, SnO2 nanoparticles are found in the mesopore and micropore of rice husk-activated carbon (RHAC) *(Ramamoorthy et al., 2020)*.[29]

$$D = \frac{k\lambda}{\beta cos\theta} (2)$$

Where, D = Crystalline size, K = shape factor(0.9), λ = wavelength of X-ray (0.15406nm), β = Full width half maxima FWHM, θ = diffraction angle

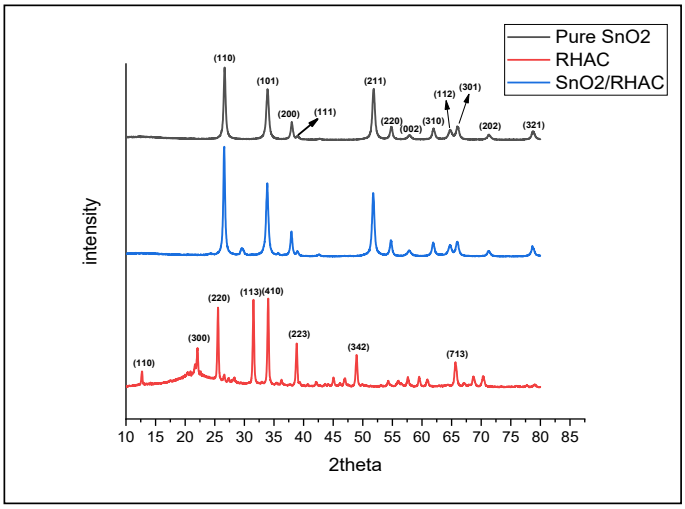

FIGURE5: XRD patterns of Pure SnO_2, RHAC, and SnO_2/RHAC

Removal of Methylene Blue

(i) Adsorption study

An adsorption study was conducted for MB removal by RHAC, pure SnO_2, and SnO_2/RHAC. The RHAC showed the highest adsorption efficiency for methylene blue at pH 10 after 180. min,91% of dye was removed as shown in Figure 6. The pure SnO_2 showed the highest removal efficiency of 56% for MB at pH 10 after 180min as shown in Figure 7,

while SnO_2/RHAC removed 90% of methylene blue at pH 7 after 180minas shown in Figure 8. The structural characteristics and surface characteristics of the MB and substance, which are regulated by pH, have a significant impact on how well the sorbent removed the dye. As a result, every modification in solution pH had an impact on the makeup of charges on MB and material surfaces, which influenced properties such as electrolyte interaction, stability, suspension rheology, and ion exchange capacity. At neutral pH,the largest proportion of removal occurred in SnO_2/RHAC in comparison to RHAC which showed the largest amount of percentage removal of 91% at pH10.[30]

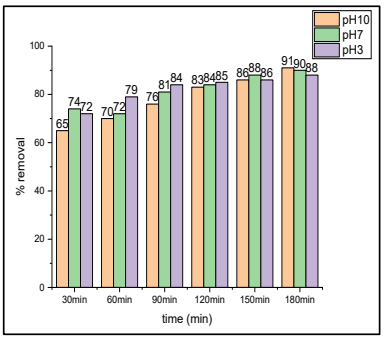

FIGURE6: % adsorption of MB on RHAC

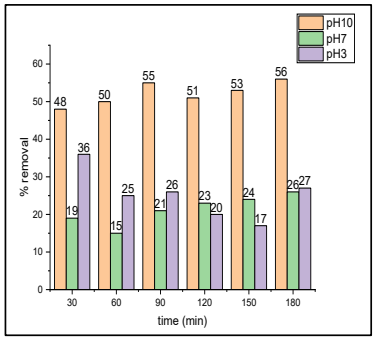

FIGURE 7:% adsorption of MB on pure SnO_2

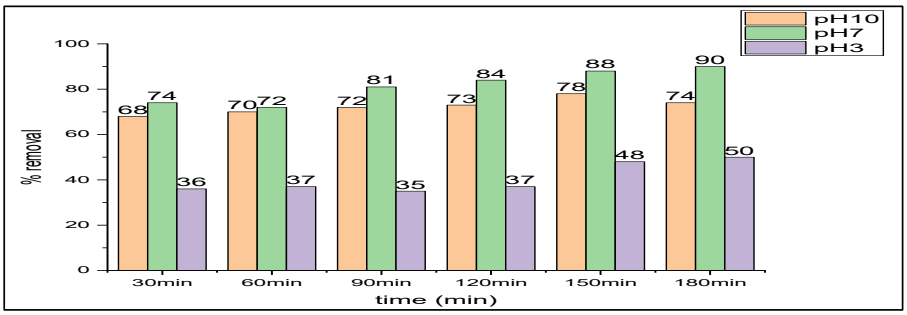

FIGURE 8:% adsorption of MB on RHAC/SnO_2

(ii) Photocatalytic study

In order to understand the role of light on the removal of MB, photocatalytic study in presence of tungsten light was carried out. SnO_2 nanoparticles removed 75% of dye at pH 10 as shown in Figure 9 (a) whereas SnO_2/RHAC showedthe highest removal efficiency of 61% at 180min in pH 10 as shown in Figure9 (b).Electrostatic interactions led to competitive sorption between H^+ ions and the cationic dye MB at lower *p*Hs, which reduced the amount of dye adsorbed onto the material and delayed the photocatalytic reaction.The results of photocatalytic degradation revealed that pure SnO_2 is more efficient at pH 10 with 75% dye degradation but at pH 3 and 7, it removed 23% and 32% of dye respectively. The composite of SnO_2 with RHAC showed less photocatalytic activity at higher pH but at pH of 3 and 7, it gave better results than pure SnO_2 with values of 46% and 45% respectively.[31]

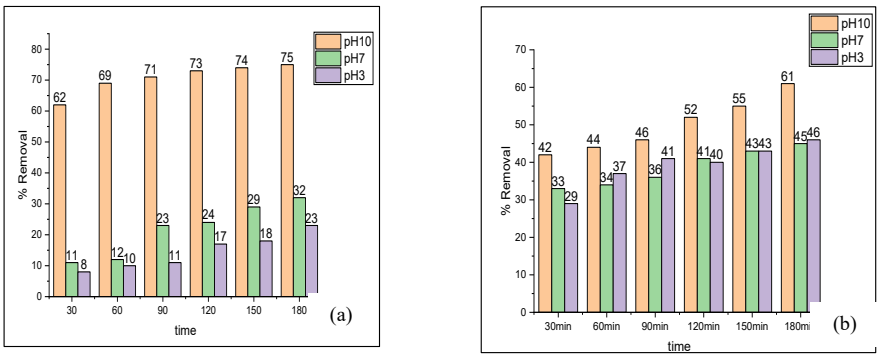

FIGURE 9 (a): Photocatalytic degradation of MB with pure SnO_2; **(b)**Photocatalytic degradation of MB with SnO_2/RHAC

CONCLUSION

This research study focuses on preparation of biochar-based material of removal of dyes from wastewater. The biochar was prepared from rice husk biomass and pyrolyzed at 800˚C in nitrogen inert environment.In order to evaluate the removal efficiency, RHAC and SnO_2composite was prepared. The composites was characterizedusing numerous types techniques such as Fourier transform infrared spectroscopy (FTIR), X-Ray diffraction (XRD), and Scanning electron microscopy (SEM).The degradation of MB was studied using the synthesized material both by adsorption and photocatalysis. The results have revealed that SnO_2 showed better removal efficiency by photocatalysis (75% at pH 10) while RHAC gave better performance at pH 10 with removal percentage of 91% by adsorption. On the contrary, the composite SnO_2/RHAC (5:1) gave lesser activity with removal percentage of 61% at pH 10 but it had more recyclability. It becomes evident that this composition was not showing synergism of adsorption (RHAC) and photocatalysis (SnO_2). More research work is required to optimize the percentage composition of composite so that better efficiency is obtained

REFERENCES

1 Khadhri N, El Khames Saad M, ben Mosbah M, Moussaoui Y, Batch and continuous column adsorption of indigo carmine onto activated carbon derived from date palm petiole, Journal of Environmental Chemical Engineering (2018), https://doi.org/10.1016/j.jece.2018.11.020

2 Liu, Bin; Gu, Jie; Zhou, Jianbin (2016). *High surface area rice husk-based activated carbon prepared by chemical activation with $ZnCl_2$, $CuCl_2$ composite activator. Environmental Progress & Sustainable Energy, 35(1), 133–140.* doi:10.1002/ep.12215

3 Zhang, Zhe; Luo, Xinsheng; Liu, Yani; Zhou, Pengxin; Ma, Guofu; Lei, Ziqiang; Lei, Lei (2015). *A low-cost and highly efficient adsorbent (activated carbon) prepared from waste potato residue. Journal of the Taiwan Institute of Chemical Engineers, 49(), 206–211.* doi:10.1016/j.jtice.2014.11.024

4 B.H. Hameed; A.T.M. Din; A.L. Ahmad (2007). *Adsorption of methylene blue onto bamboo-based activated carbon: Kinetics and equilibrium studies., 141(3), 819–825.* doi:10.1016/j.jhazmat.2006.07.049

5 Chen Y-D, Chen W-Q, Huang B, Huang M-J (2013) Process optimization of K2C2O4-activated carbon from kenaf core using Box–Behnken design. Chem Eng Res Des 91:1783–1789. https://doi.org/10.1016/j.cherd .2013.02.024

6 Cui X, Jia F, Chen Y, Gan J (2011) Influence of single-walled carbon nanotubes on microbial availability of phenanthrene in sediment. Ecotoxicology 20:1277–1285. https://doi.org/10.1007/s1064 6-011-0684-3

7 Gao, Jj., Qin, Yb., Zhou, T. et al. Adsorption of methylene blue onto activated carbon produced from tea (Camellia sinensis L.) seed shells: kinetics, equilibrium, and thermodynamics studies. J. Zhejiang Univ. Sci. B 14, 650–658 (2013). https://doi.org/10.1631/jzus.B12a0225

8 Guo, Nannan; Li, Min; Wang, Yong; Sun, Xingkai; Wang, Feng; Yang, Ru (2016). *Soybean root-derived hierarchical porous carbon as an electrode material for high performance supercapacitors in ionic liquids. ACS Applied Materials & Interfaces, (), acsami.6b11162–.* doi:10.1021/acsami.6b11162

9 Heidarinejad, Zoha; Rahmanian, Omid; Fazlzadeh, Mehdi; Heidari, Mohsen (2018). *Enhancement of methylene blue adsorption onto activated carbon prepared from Date Press Cake by low-frequency ultrasound. Journal of Molecular Liquids, 264(), 591–599.* doi:10.1016/j.molliq.2018.05.100

10 Huang Y, Zhao G (2016) Preparation and characterization of activated carbon fibers from liquefied wood by KOH activation. Holzforschung 70:195–202. https://doi.org/10.1515/hf-2015-0051

11 Islam, M. Azharul; Benhouria, A.; Asif, M.; Hameed, B.H. (2015). *Methylene blue adsorption on factory-rejected tea-activated carbon prepared by the conjunction of hydrothermal carbonization and sodium hydroxide activation processes. Journal of the Taiwan Institute of Chemical Engineers, 52(), 57–64.* doi:10.1016/j.jtice.2015.02.010

12 Islam, Md. Azharul; Ahmed, M.J.; Khanday, W.A.; Asif, M.; Hameed, B.H. (2017). *Mesoporous activated carbon prepared from NaOH activation of rattan (Lacosperma secundiflorum) hydrochar for methylene blue removal. Ecotoxicology and Environmental Safety, 138(), 279–285.* doi:10.1016/j.ecoenv.2017.01.010

13 Jolly G, Dupont L, Aplincourt M, Lambert J (2006) Improved Cu and Zn sorption on oxidized wheat lignocellulose. Environ Chem Lett 4:219–223. https://doi.org/10.1007/s10311-006-0051-4

14 Khadhri N, Saad MEK, ben Mosbah M, Moussaoui Y (2019) Batch and continuous column adsorption of indigo carmine onto activated carbon derived from date palm petiole. J Environ Chem Eng 7:102775. https://doi.org/10.1016/j.jece.2018.11.020

15 Kaur P, Kaur P, Kaur K. Adsorptive removal of imazethapyr and imazamox from aqueous solution using modified rice husk. *Journal of Cleaner Production*. 2020. 20;244: 118699.

16 Lv, Songlei; Li, Chunxi; Mi, Jianguo; Meng, Hong A functional activated carbon for efficient adsorption of phenol derived from pyrolysis of rice husk, KOH-activation, and EDTA-4Na-modification. *Applied Surface Science,* 2020*, 145425.* doi:10.1016/j.apsusc.2020.145425

17 Mahamad, Mohammed Nabil; Zaini, Muhammad Abbas Ahmad; Zakaria, Zainul Akmar (2015). *Preparation and characterization of activated carbon from pineapple waste biomass for dye removal. International Biodeterioration & Biodegradation, 102(), 274–280.* doi:10.1016/j.ibiod.2015.03.009

18 Maneerung, T., Liew, J., Dai, Y., Kawi, S., Chong, C., Wang, C-H., Activated carbon derived from carbon residue from biomass gasification and its application for dye adsorption: kinetics, isotherms and thermodynamic studies, Bioresource Technology (2015), doi: http://dx.doi.org/10.1016/j.biortech.2015.10.047

19 Md Sumon Reza, Cheong Sing Yun, Shammya Afroze, Nikdalila Radenahmad, Muhammad S. Abu Bakar, Rahman Saidur, Juntakan Taweekun & Abul K. Azad (2020) Preparation of activated carbon from biomass and its applications in water and gas purification, a review, Arab Journal of Basic and Applied Sciences, 27:1, 208-238, DOI: 10.1080/25765299.2020.1766799

20 Nguyen, Trong Nghia; Le, Phuoc Anh; Phung, Viet Bac T. (2020). *Facile green synthesis of carbon quantum dots and biomass-derived activated carbon from banana peels: synthesis and investigation. Biomass Conversion and Biorefinery, (), –.* doi:10.1007/s13399-020-00839-2

21 Prauchner MJ, Sapag K, Rodríguez-Reinoso F (2016) Tailoring biomass-based activated carbon for CH4 storage by combining chemical activation with H3PO4 or ZnCl2 and physical activation with CO2. Carbon 110:138–147. https://doi.org/10.1016/j. carbon.2016.08.092

22 Ramamoorthy, M.; Ragupathy, S.; Sakthi, D.; Arun, V.; Kannadasan, N. (2020). *Synthesis of SnO2 loaded on corn cob activated carbon for enhancing the photodegradation of methylene blue under sunlight irradiation. Journal of Environmental Chemical Engineering, (), 104331–.* doi:10.1016/j.jece.2020.104331

23 Ru-Ling Tseng; Szu-Kung Tseng (2006). *Characterization and use of high surface area activated carbons prepared from cane pith for liquid-phase adsorption. , 136(3), 671–680.* doi:10.1016/j.jhazmat.2005.12.048

24 Samsuri A, Sadegh-Zadeh F, Seh-Bardan B (2014) Characterization of biochars produced from oil palm and rice husks and their adsorption capacities for heavy metals. Int J Environ Sci Technol 11:967–976. https://doi.org/10.1007/s13762-013-0291-3

25 Schröder, E., Thomauske, K., Weber, C., Hornung, A. and Tumiatti, V., 2007. Experiments on the generation of activated carbon from biomass. *Journal of analytical and applied pyrolysis*, *79*(1-2), pp.106-111.

26 Youssef A, Ahmed A, El-Bana U (2012) Adsorption of cationic dye (MB) and anionic dye (AG 25) by physically and chemically activated carbons developed from rice husk. Carbon Lett 13:61–72.https://doi.org/10.5714/CL.2012.13.2.061

27. Darwish, M.A., Trukhanov, A.V., Senatov, O.S., Morchenko, A.T., Saafan, S.A., Astapovich, K.A., Trukhanov, S.V., Trukhanova, E.L., Pilyushkin, A.A., Sombra, A.S.B. and Zhou, D., 2020. Investigation of AC-measurements of epoxy/ferrite composites. Nanomaterials, 10(3), p.492.

28. Bashir, S., Sharma, V., Lgaz, H., Chung, I.M., Singh, A. and Kumar, A., 2018. The inhibition action of analgin on the corrosion of mild steel in acidic medium: A combined theoretical and experimental approach. Journal of Molecular Liquids, 263, pp.454-462.

29. Trukhanov, A.V., Astapovich, K.A., Turchenko, V.A., Almessiere, M.A., Slimani, Y., Baykal, A., Sombra, A.S.B., Zhou, D., Jotania, R.B., Singh, C. and Zubar, T.I., 2020. Influence of the dysprosium ions on structure, magnetic characteristics and origin of the reflection losses in the Ni–Co spinels. Journal of Alloys and Compounds, 841, p.155667.

30. Prakash, C., Singh, S., Pruncu, C.I., Mishra, V., Królczyk, G., Pimenov, D.Y. and Pramanik, A., 2019. Surface modification of Ti-6Al-4V alloy by electrical discharge coating process using partially sintered Ti-Nb electrode. Materials, 12(7), p.1006.

31. Bharany, S., Sharma, S., Badotra, S., Khalaf, O.I., Alotaibi, Y., Alghamdi, S. and Alassery, F., 2021. Energy-efficient clustering scheme for flying ad-hoc networks using an optimized LEACH protocol. Energies, 14(19), p.6016.